Accepted Manuscript

Pharmacokinetic study based on a matrix-assisted laser desorption/ionization quadrupole ion trap time-of-flight imaging mass microscope combined with a novel relative exposure approach: A case of octreotide in mouse target tissues

Tai Rao, Yuhao Shao, Naoki Hamada, Yanmin Li, Hui Ye, Dian Kang, Boyu Shen, Xinuo Li, Xiaoxi Yin, Zhangpei Zhu, Haofeng Li, Lin Xie, Guangji Wang, Yan Liang

PII: S0003-2670(16)31406-4

DOI: 10.1016/j.aca.2016.11.056

Reference: ACA 234927

To appear in: *Analytica Chimica Acta*

Received Date: 31 August 2016

Revised Date: 3 November 2016

Accepted Date: 24 November 2016

Please cite this article as: T. Rao, Y. Shao, N. Hamada, Y. Li, H. Ye, D. Kang, B. Shen, X. Li, X. Yin, Z. Zhu, H. Li, L. Xie, G. Wang, Y. Liang, Pharmacokinetic Study based on a Matrix-Assisted Laser Desorption/ionization Quadrupole Ion Trap Time-of-flight Imaging Mass Microscope Combined with a Novel Relative Exposure Approach: A Case of Octreotide in Mouse Target Tissues, *Analytica Chimica Acta* (2017), doi: 10.1016/j.aca.2016.11.056.

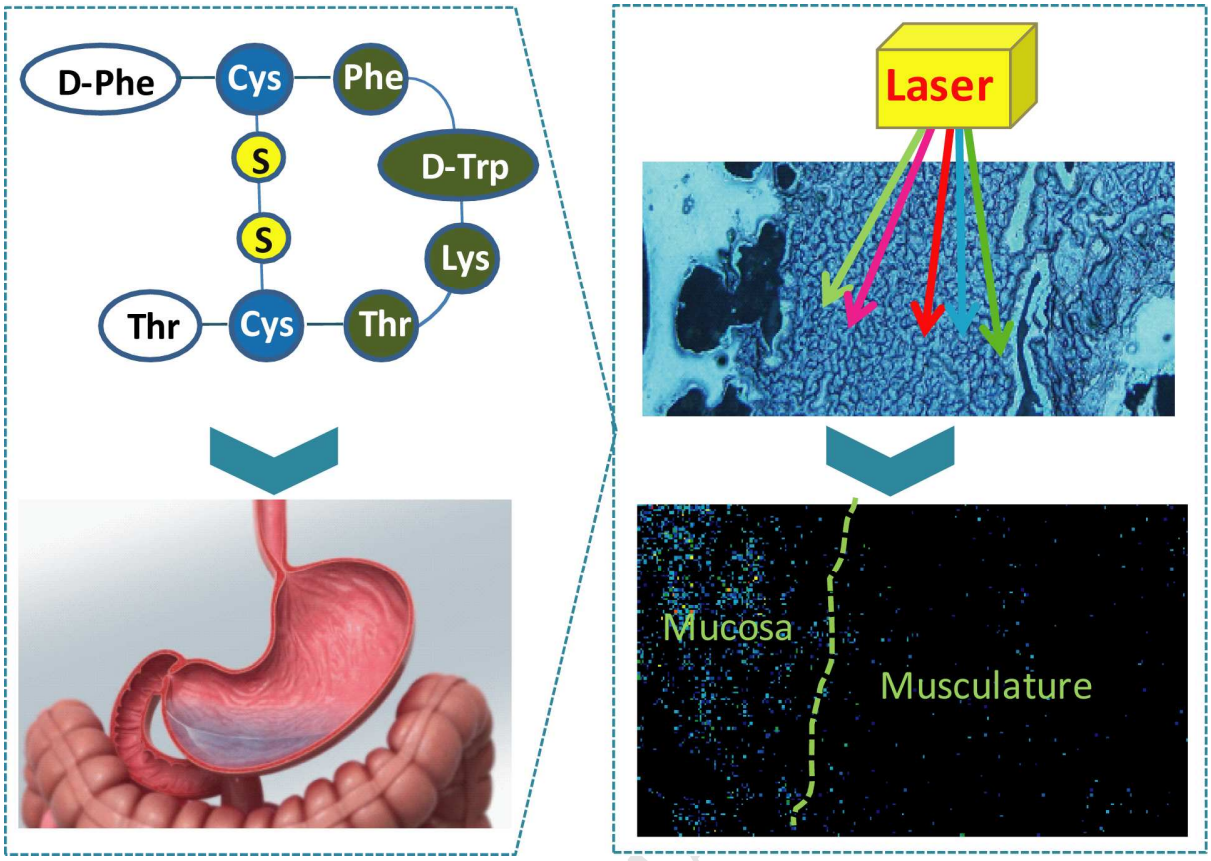

Pharmacokinetic Study based on a Matrix-Assisted Laser Desorption/ionization Quadrupole Ion Trap Time-of-flight Imaging Mass Microscope Combined with a Novel Relative Exposure Approach: A Case of Octreotide in Mouse Target Tissues

Tai Rao[1a], Yuhao Shao[1a], Naoki Hamada[b], Yanmin Li[b], Hui Ye[a], Dian Kang[a], Boyu Shen[a], Xinuo Li[a], Xiaoxi Yin[a], Zhangpei Zhu[a], Haofeng Li[a], Lin Xie[a], Guangji Wang[**a], Yan Liang[*a]

a. Key Lab of Drug Metabolism & Pharmacokinetics, State Key Laboratory of Natural Medicines, China Pharmaceutical University, Tongjiaxiang 24, Nanjing 210009, P.R. China

b. Shimadzu China Mass Spectrometry Center, No. 16 Chao Yang Men Wai Street, Chaoyang District, Beijing 100020, P.R. China

*Corresponding author. Tel. : +86 25 83271060; fax: +86 25 83271060.

**Co-corresponding author. Tel.: +86 25 83271128; fax: +86 25 83302827.

E-mail addresses: liangyan0679@163.com

[1] These two authors contributed equally to this work.

ABSTRACT

Application of imaging mass spectrometry in drug pharmacokinetics remains challenging due to its weak quantitative capability. Herein, an imaging mass microscope (iMScope), equipped with an optical microscope, an atmospheric pressure ion-source chamber for matrix-assisted laser desorption/ionization (AP-MALDI) and a hybrid quadrupole ion trap time-of-flight (QIT-TOF) analyzer, was first validated and applied to visualize drug disposition *in vivo*. The distribution and elimination rate of the therapeutic peptide octreotide, a long-acting analogue of the natural hormone somatostatin, was first calculated based on the data determined by iMScope system combining a novel relative exposure strategy. Microspotted pixel-to-pixel quantitative iMScope provided a relative amount of octreotide presented in a thin stomach/intestinal section while preserving its original spatial distribution. The images of dosed mouse stomach clearly demonstrated the transport process of octreotide from the mucosal layer to the muscle side. More importantly, octreotide was found to eliminate from the intestines rapidly, the absorption peak time (T_{max}) appeared at 40 min and the half-life time ($t_{1/2}$) was calculated as 37.7 min according to the elimination curves. Comparisons to the LC-MS/MS data adequately indicated that the quantification approach and methodology based on the iMScope was reliable and practicable for drug pharmacokinetic study.

Keywords: IMScope; Relative exposure; Octreotide; Distribution; Elimination

1. Introduction

Mass spectrometry imaging (MSI) has increasingly emerged as an effective tool to survey the distribution of small molecule compounds and biological macromolecules in flat surgical tissues, such as biological tissue specimens, plant slices or inorganic materials [1-5]. Prominent progress has been obtained in the past few years, not only with regard to the performance of the device, such as the sensitivity, lateral resolution and mass accuracy, but also to applications in qualitative and quantitative analysis for chemistry, biology and medicine [6-8]. In the past three years, MALDI/LDI-Fourier transform ion cyclotron resonance (FTICR)-MS incorporating certain specific features namely, high mass resolution, high molecular mass accuracy and high spatial resolution has been frequently used in the research fields of proteomics, lipidomics, plant tissues, *etc* [9-12]. Not long ago, a novel surface plasmon resonance imaging-matrix assisted laser desorption ionization mass spectrometry imaging (SPRi-MALDI MSI) was used to provide quantitative and qualitative images of intact proteins contained within a tissue section [1]. More recently, in a study just published in the Analytical Chemistry journal, Carter, *et al.* developed an inflation-fixation MALDI-MSI method, which could be applied to lipidomic investigations of whole lung samples and resected biopsy specimens [13]. Besides, the MALDI-MSI is being applied to the identification and the spatial localization of small molecules in bio-fluid or animal tissues [14-17]. Despite its clear promise, the application of MALDI IMS in pharmacokinetic research is still in its infancy to date and is facing critical obstacles in the absolute quantitative capability due to tissue heterogeneity and ionization suppression effects [18-22]. Besides, the image pixel size could be another limitation when we observe the drug disposal process microscopically [23, 24].

Liquid chromatography combined single-stage quadrupole MS (LC-MS), as well as triple-stage quadrupole MS (LC-MS/MS), are commonly used by drug researchers for pharmacokinetic studies owing to their excellent sensitivity, high specificity, low cost and relatively small size [25-27]. However, the dosed tissues must undergo a homogenate and complex purification process when the LC-MS or LC-MS/MS systems was used in the drug distribution research, and the specific localization of the drug at the organelle-level cannot be

distinguished precisely and the “microscopic” transport process of the drug in internal tissue is largely ignored during the tissue homogenization prior to performing LC-MS/MS analysis [18]. In recent years, a novel mass microscope (iMScope) developed by Shimadzu Corporation (Shimadzu, Kyoto, Japan), equipped with an atmospheric pressure ion-source chamber for matrix-assisted laser desorption/ionization (AP-MALDI) and a quadrupole ion trap time-of-flight (QIT-TOF) analyzer, has great shown promise in simultaneously assessing the spatial distribution and molecular profiling in a non-targeted manner [28-30]. Particularly, the optical microscope combined with the mass spectrometer permitted a precise determination of the regions of interest (ROIs) via magnifying $\times 10$ to $\times 40$ by the CCD camera. An ultraviolet laser tightly focused with a triplet lens was used to achieve high spatial resolution images with a micrometer pixel size. The combination of a tandem quadrupole ion trap and TOF, featuring both the MS^n capability of ion-trap and the capability to perform high-resolution and high-accuracy mass measurement based on TOF, can achieve excellent sensitivity, good repeatability and stable mass accuracy over long periods of time [31-33]. Collectively, these characteristics imply that iMScope may effectively overcome the obstacles which appeared in the pharmacokinetic assay based on the other MALDI-MSI techniques previously reported. In the present study, the potential of iMScope in drug pharmacokinetic research was systematically investigated. Firstly, a novel and facile assay was developed to evaluate the spatial resolution of the mass microscope in iMScope imaging based on the analysis of samples wrapped in 2, 5-dihydroxybenzoic acid (DHB) crystal. Subsequently, a “two-step matrix application” method, which combined with matrix sublimation and airbrushing, was chosen as the optimum matrix coating way to overcome incomplete matrix crystal formation and an inhomogeneous matrix layer. Then, the quantitative ability of iMScope, with respect to spatial resolution, linearity, sensitivity and precision, was investigated via continual measuring analytes in fresh tissue slices at different concentrations independent of isotope-labeled internal standard. More importantly, a relative exposure approach (REA) independent of absolute quantitative analysis was developed based on calculating the pharmacokinetic parameters according to the changing trend of peak intensity or peak intensity ratio (analytes / IS) to overcome the tough problem in pharmacokinetic research based on iMScope. Bioactive peptide octreotide, a long-acting analogue of the natural hormone

somatostatin, has been widely used in the clinic to control variceal hemorrhage and has been demonstrated to be effective in preventing gastrointestinal bleeding [34, 35]. The pharmacokinetic study for octreotide in the mouse gastrointestinal tract is of great significance for clarifying the mechanism of the pharmacological effects and setting the dosing interval. In our previous study, rat plasma pharmacokinetics was studied based on LC-MS/MS combining protein precipitation and impurity extraction technique [36]. However, the distribution and elimination of octreotide in animal tissues is not fully understood to date. Herein, using octreotide as the model compound, a novel, validated and facile assay was successfully developed for drug distribution study based on iMScope.

Using the presently developed approach and methodology, the transport process of octreotide from stomach mucosa layer to the muscle side was clearly visualized, and the pharmacokinetic parameters (T_{max} and $t_{1/2}$) of octreotide in mouse stomach and intestines were calculated according to the relative amount of octreotide in mouse gastrointestinal tract. The results showed that the absorption peak time (T_{max}) of octreotide in mouse stomach and intestinal appeared at 10 min and 40 min, respectively. The half-life time ($t_{1/2}$) in stomach and intestinal was calculated as 28.0 min 37.7 min according to the changing trend of peak intensity ratio (octreotide / IS). These parameters have great significance in designing a rational clinical therapeutic regimen for octreotide. More importantly, the quantitative performance of MALDI-TOF-MSI assay was further verified by comparison with a well-established LC-MS/MS assay, and the data indicated that the tissue concentration-time curves of octreotide determined by iMScope agreed well with those measured by LC-MS/MS. Thus, the presently developed strategy based on iMScope could be widely applied in drug pharmacokinetic study.

2. Experimental and methods

2.1. Materials and Instruments

MALDI grade α-Cyano-4-hydroxycinnamic acid (CHCA), sinapinic acid (SA) and 2, 5-dihydroxybenzoic acid (DHB) were purchased from Sigma-Aldrich (St. Louis, MO, USA). Octreotide acetate and lanreotide acetate were purchased from Shanghai Guang Rui

Biotechnology Co., Ltd (Shanghai, China). Porcine skin gelatin and trifluoroacetate (TFA) were purchased from Sigma-Aldrich (St. Louis, MO, USA). HPLC-grade acetonitrile and methanol were purchased from Merck Company (Darmstadt, Germany). Ultra-pure grade (18 MΩ) water was prepared by a Milli-Q system (Millipore Corporation, Billerica, MA). Electrically-conductive glass slides (Corning® Boro-Aluminosilicate Glass Products, CB-50IN-S111) were purchased from Delta-Technologies (http://www.delta-technologies.com/products.asp?C=1).

2.2. Animal Study

Balb/c mice (male, 3 weeks) were purchased from Shanghai Super -- B&K Laboratory Animal Corp. Ltd. (Shanghai, China) and kept in an environmentally controlled breeding room for at least 3 days before experimentation. All experimental procedures on animals were performed in accordance with the Guidelines of Chinese Association for Laboratory Animal Science and with the approval of the Animal Experimentation Committee at China Pharmaceutical University. After intragastrical (i.g.) administration of octreotide at a dose of 50 mg/kg, the mice were sacrificed at 10, 20, 40, 60, 120, 240 and 360 min under anesthesia (n=3). The stomach and intestinal tissues were then removed from the mice and normal saline was used for cleaning the contents of the gastrointestinal tract. In order to maintain the tissue structural integrity and histological representation as far as possible, 100 mg/ml of gelatin was used to fill the cavity of the stomach and intestines. Finally, all the tissues were flash-frozen in powdered dry ice and then stored at −80 °C until use.

2.3. Tissue Sectioning and Matrix Coating

Frozen 10 μm of mouse stomach and intestinal sections were sliced at −20 °C with a cryomicrotome (Leica CM1950, Nussloch, Germany) and then thaw-mounted onto electrically-conductive glass slides. Subsequently, matrix coating modes were optimized via comparing the signal/noise (S/N) of octreotide produced under 4 possible ways of matrix coating as follows: **(1) Sublimation**: the electrically-conductive glass slide bearing specimen (blank stomach slice spiked with 5 pmol of octreotide) was installed in a sample holder, which was then imbedded in a vacuum deposition system (SVC-700TMSG iMLayer, Sanyu Electron, Tokyo, Japan). A matrix holder was filled with approximately 50 mg of matrix powder (DHB, CHCA or

SA) and the sample holder and matrix bracket were positioned with 8 cm distance. The matrix power was then heated to the boiling point of the matrix crystals (203°C for DHB, 250 °C for CHCA, and 400 °C for SA) and the vapor covered the specimen surface for 8 min. The vacuum pressure of the chamber was maintained at 10^{-4} Pa in the process of sublimation. **(2) Sublimation & recrystallization**: the detailed procedures are divided into 5 steps: (i) An electrically-conductive glass slide bearing the specimen (blank stomach slice spiked with octreotide) was treated with the CHCA matrix based on the sublimation method; (ii) Put a piece of filter paper into a sealed container after dipping in methanol together with the glass slide, and keep a distance of 1 cm between the filter paper and the glass slide; (iii) Heat the container for 10 min at 60 °C using a water-bath; (iv) Remove the glass slide from the closed container, and then put it into a vacuum dryer to vaporize the solvent for 5 min. **(3) Airbrushing:** matrix solution (10 mg/ml) was prepared by dissolving matrix power in acetonitrile and distilled water (all containing 0.1 % formic acid; FA) at a ratio of 1:1. The matrix solution (1 ml) was added to the capacity of an artist's airbrush (MR. Linear Compressor L7/PS270 Airbrush, GSI Creos, Tokyo, Japan). The distance between the tip of the airbrush and the tissue surface was about 8 cm. For the first 3 cycles, the matrix was airbrushed for 2 s at 60 s intervals and, in the following 7 cycles, the matrix was continuously sprayed for 1.0 s at 30 s intervals. The glass slide was then placed in a vacuum dryer to vaporize the solvent for 5 min. **(4) Sublimation & Airbrushing:** a "two-step matrix application", which combined with sublimation and airbrushing, was used to coat matrix for tissue sections. In the first step, the matrix was coated on the glass slide uniformly in the vacuum chamber of SVC-700TMSG iMLayer under the same conditions described in the **"(1) Sublimation"** part. In the second step, matrix (10 mg/mL) solution was sprayed onto the glass slide for 10 cycles using the artist's airbrush according to the procedures described in the "**(3) Airbrushing"**.

2.4. Imaging MS Analysis based on iMScope

An iMScope (Shimadzu, Japan) instrument, a hybrid IT-TOF mass spectrometer combining an optical microscope and atmospheric pressure matrix-assisted laser desorption/ ionization system, was used to acquire the imaging MS data. One of the most critical processes in MSI is the

creation of the region of interest (ROI). The optical microscope embedded in the iMScope permitted us to precisely choose the relevant tissue region prior to performing data acquisition. An ultraviolet laser, tightly focused with a triplet lens, was used to ensure high spatial resolution. Based on the advanced configuration above, a tissue ROI was freely selected via a charge-coupled device (CCD) camera (magnification, ×1.25, ×2.5, ×5, ×10, ×20, and ×40; Olympus Corporation, Tokyo, Japan) and the imaging area was then defined according to the maximum imaging point under a scan pitch of 5 to 20 μm. Foci and observation points were controlled with a joystick, and the XYZ stage (Kohzu Precision, Kanagawa, Japan) on which the electrically-conductive glass slide was fixed. The XYZ coordinates, with position-feedback scales, immediately displayed the ROIs to make position reproducibility possible on a submicrometer order. The tissue slices were then irradiated by a focused laser beam in synchrony with stage scanning. The laser in the iMScope system was a diode-pumped 355 nm Nd:YAG laser (Shimadzu Corporation, Kyoto, Japan) and operated under the following parameters: frequency, 500 Hz; laser intensity, 25.0; pulse width, 5 ns. All the experiments in this work were conducted with the minimum irradiation diameter, and the irradiated the tissue surface with 50 shots (repetition rate; 500 Hz) for each pixel.

IT-TOF MS, with complementary capacity in providing multistage fragmentations and accurate mass measurements, can provide an advantage in reliable qualitative and quantitative analysis for biomolecules. The parameters of IT-TOF MS were set as follows: ion polarity, positive; mass range, 950-1200; sample voltage, 3.5 kV; detector voltage, 1.90 kV. The imaging MS Solution Version 1.12.26 software (Shimadzu, Tokyo, Japan) was used to control the instrument, and the data acquisition, visualization and quantification was also performed by the same software.

2.5. Preparation of Calibration Specimen

Calibration standards (2, 5, 10, 20 and 40 pmol/μl) of octreotide and an internal standard (10 pmol/μl) of lanreotide were prepared in acetonitrile and distilled water (all containing 0.1 % of FA) at a ratio of 1:1 by independent dilution of the drug stock solution (10.0 mg/ml of octreotide in acetonitrile). Then, 0.5 μl of the calibration standards were deposited onto a blank tissue (stomach

and intestinal) section by a micropipettor. A total of five microspots were deposited for each concentration on the calibration curve. Also, the quality control solution (5 pmol/µl) was used to determine the precision of the method.

2.6. Homogenization and Absolute Quantification Analysis of Octreotide by LC-MS/MS.

The dosed and control gastrointestinal tissues were cut (~50 mg) and homogenized in 1ml of water (~50 mg/ml). After precipitating proteins, the tissue specimens were analyzed using a fully-validated LC-MS/MS assay [36]. Calibration standard solutions of octreotide (2, 5, 10, 20 and 40 pmol/µl) and IS solution (10 pmol/µl) were spiked into 75 µl of the control tissue homogenate. Only the internal standard was spiked into 75 µl of the dosed tissue homogenates. Then 200 µl of acetonitrile was added to precipitate protein. After mixing for 30 s and centrifugation at 15,000 g for 10 min, 200 µl of the supernatant was transferred to clean Eppendorf tubes. Then, 500 µl of dichloromethane and 200 µl of water were added to remove endogenous interferences. After vortex-mixing for 30 s and centrifugation at 40,000 g for 5min, 5 µl of supernatant was injected into the Shimadzu 8050 LC-MS/MS system (Tokyo, Japan). Chromatographic separation for octreotide and IS was performed on a Sepax Bio-C18 column (150 mm × 2.1 mm, 5 µm, 300 Å) using 0.1 % formic acid (solvent A) and methanol (solvent B) as mobile phase with a flow rate at 0.2 ml/min. The gradient was as follows: an isocratic elution of 5 % solvent B for the initial 1.0 min, followed by linear increasing from 5% to 80% of solvent B from 1 to 6 min, hold for 2 min, linearly decreasing from 80% to 10% in 1 min, and hold for 3 more minutes. Quantitative analysis was performed using multiple reactions monitoring (MRM) mode by monitoring the precursor ion to product ion transitions of *m/z* 510.5 → 120.1 for octreotide and *m/z* 548.8→170.2 for lanreotide (IS). The ionspray voltage and source temperature were maintained at 4000 V and 300 ◦C, respectively. The collision energy for octreotide and IS was 38 eV. LabSolutions LCMS Ver.5.6 software (Shimadzu, Japan) was used for the instrument control and data processing.

3. RESULTS AND DISCUSSION

3.1. Evaluation of Spatial Resolution of iMScope

MSI is a powerful tool to study the spatial distribution of single or multiple molecules on surfaces and it would be critical to investigate if the intensity of some designated mass signal significantly differs among some regions of interest (ROIs). Certainly, the accuracy of a test to detect distribution differences is greatly influenced by the number of pixels and spatial resolution [18, 19]. A higher spatial resolution should lead to a higher reliability and vice versa. In the present study, a novel and facile assay was developed to evaluate the effective spatial resolution of the iMScope based on the analysis of octreotide wrapped in a DHB crystal. First, 20 mg of DHB, 100 ng of octreotide and 500 ng of lanreotide (internal standard, IS) were dissolved in 1ml of acetonitrile and distilled water (all containing 0.1 % of FA) at a ratio of 1:1. The matrix solution was then added to the cavity of an artist's airbrush and continuously sprayed onto an electrically-conductive glass slide tagged with 10 μm of mouse stomach sections for 10 cycles with 30 s intervals. After vaporizing the solvent in a vacuum dryer, the electrically-conductive glass slide was installed in the iMScope and the imaging area was then defined with the help of the CCD camera with magnification of 40X. The imaging MS scanning was carried out with 5-μm pixel size. As shown in **Fig. 1a**, DHB crystals could be clearly observed with the typical shape of a willow leaf [37]. **Fig. 1b** and **Fig. 1c** showed the ion images of the octreotide and lanreotide generated by iMScope at *m/z* 1019.44 and 1096.47, respectively. Obviously, the images of octreotide and lanreotide made a perfect match with the shapes of DHB crystals. And clear-edge images with 1 pixel widths (5 × 5μm) were obtained along the edge of the crystal. Therefore, the effective spatial resolution for the vertical and horizontal orientations in LDI imaging was 5 μm or less.

3.2. Selection of Internal Standard and Suitable Matrices

An ideal IS should be the stable isotope-labeled intact peptide / protein during qualitative and quantitative analysis of a therapeutic peptide or protein [38, 39]. However, it was impractical in the present case due to synthesis challenges and time & cost concerns. Lanreotide, a structural analogue of octreotide, was used as the internal standard due to the similarity in their molecular

weight, amino acid sequence and ionization characteristics. The structures and MS spectrum of octreotide and lanreotide are shown in **Fig. 2**.

The MALDI matrixes, aromatic compounds of low molecular mass, which are crucial for optimal signal-to-noise levels and the quality of data, were used to enhance the ionization efficiency and prevent the analytes from degrading [40]. Owing to the specific ionization property of the individual matrix, the selection of a suitable matrix is understandably critical to MALDI MS. In the present study, DHB, CHCA and SA were used to screen the optimum matrix via studying their abilities to form hydrogen adducts onto analytes, and the matrix solution was prepared by dissolving 20 mg of matrix standard (DHB, CHCA or SA), 100 ng of octreotide and 500 ng of lanreotide (IS) in 1ml of acetonitrile and distilled water (all containing 0.1 % of FA) at a ratio of 1:1. This mixture solution was then added to the cavity of the artist's airbrush and continuously sprayed on an electrically-conductive glass slide tagged with 10 μm mouse stomach sections for 10 cycles with 30 s intervals. After vaporizing the solvent in a vacuum dryer, the electrically-conductive glass slide was installed in the iMScope and the imaging area was then defined with the help of the CCD camera with magnification of 40X. As shown in **Fig. 1a** and **Fig. 1b,** large crystals of DHB were characterized by non-uniform distribution associated with the disappearance of ion signals of the analytes, which failed to be wrapped by the matrix. Contrary to what was observed for DHB single crystals, no obvious crystallization was found using the CCD camera with magnification at 40X after spraying CHCA and SA on the tissue section (**Fig. 1d** and **Fig. 1f**). The ion signal of octreotide generated by iMScope was evenly scattered over the tissue sections (**Fig. 1e** and **Fig. 1g**). The average ion signal intensity of the octreotide image in **Fig. 1g** (produced using SA as the hydrogen donor) was much lower than that in **Fig. 1e** (produced using CHCA as the hydrogen donor). Thus, the determined hydrogen-donating ability of CHCA was much higher than that of SA. According to the findings above, CHCA was confirmed to be the most suitable matrix for the analysis of octreotide based on iMScope.

3.3. Screening of Matrix Coating Mode

To obtain the ideal sensitivity, the matrix coating mode was optimized via comparing the signal intensity generated under 4 different matrix coating modes at the same concentration of

octreotide. As mentioned in the experimental section, 4 different matrix coating ways were adopted for the pretreatment of the tissue specimen containing 5 pmol of octreotide: (1) sublimation, (2) sublimation & recrystallization, (3) airbrushing, (4) sublimation & airbrushing. As depicted in **Fig. 3,** the ionization efficiencies of the matrix coating modes were ranked according to the average ion signal intensity as follows: sublimation & airbrushing **(Fig. 3D)** > airbrush **(Fig. 3C)** > sublimation & recrystallization **(Fig. 3B)** > sublimation **(Fig. 3A)**. Similar to our research, Shimma, *et al.* had reported that the "two-step matrix application" method, which combined with matrix sublimation and airbrushing, could overcome incomplete matrix crystal formation and an inhomogeneous matrix layer, and was proved to be a promising break-through for achieving highly sensitive and reproducible MSI experiments [41, 42]. Taken together, sublimation & airbrushing was chosen as the matrix coating method for further experiments. In the spectrum of octreotide, the protonated molecule ion $[M+H]^+$ of octreotide at *m/z* 1019.44 was dominated in the MS spectrum. The potassium adduct ion $[M+K]^+$ at *m/z* 1057.40 could also be clearly distinguished from other ions, and the sodium adduct ion $[M+Na]^+$ at *m/z* 1041.41 was also detected, though very weakly.

3.4. Quantitative Ability of iMScope.

Firstly, the specificity performance of iMScope was evaluated by imaging octreotide and IS in drug-free mouse stomach and intestine. As shown in **Fig. S1**, the background noise was very low and no obvious interference existed in the images of octreotide (*m/z* 1019.44) and IS (*m/z* 1096.47). Another set of experiments was done to investigate the dynamic range of the iMScope. The calibration curves were generated by plotting the average intensity ratio of the precursor ion of octreotide to the manually corrected intensity of the IS (*m/z* 1019.44 / 1096.47) versus the concentration of octreotide spotted on the blank tissue section (5 microspots for each concentration). The microspots on the stomach and intestinal tissue sections had a diameter of 1.72 ± 0.10 mm and were used to define the pixels in the subsequent MSI experiment. The calibration curves of octreotide were linear in average intensity over the concentration range of 1.0 - 20.0 pmol in the mouse stomach slice, with a correlation coefficient $r > 0.999$, and the standard deviation (RSD) of the slope was less than 15 %. A representative result of the linear relation test

has been shown in **Fig. 4**. Similarly, the linear positive correlation was notable between signal intensity and the amount of octreotide that deposited on the intestinal slice, and the correlation coefficient r was 0.9999 (**Fig. S2 and Fig. S3**), which illustrated that the iMScope is suitable for quantitative analysis. Furthermore, the precision of the present assay was initially investigated via determining the average intensity ratio of octreotide and IS in four sections of blank stomach tissue covered by the same concentration of the analytes. The precision was measured by the relative standard deviation values (RSD %) to verify the repeatability. As shown in **Fig. 5,** the overall average intensity ratios of these regions were 0.3759, 0.3626, 0.3866 and 0.3787, respectively. The relative standard deviations of the measurements from each tissue section were 3.20 %. These data indicated that there was not a no significant difference among the intensity ratios of octreotide and IS detected from different batches of tissue sections by iMScope.

3.5. Quantitative Observation of the Spatial Distribution and Elimination of Octreotide from Mucosa to Musculature in Mouse Stomach.

As a common practice, drug distribution was studied "macroscopically" via measuring the drug concentration in animal tissue after homogenizing part of the tissues based on the LC-MS or LC-MS/MS systems. However, the specific localization of the drug within tissue substructures cannot be distinguished after tissue homogenization although HPLC-MS has been successful in performing absolute quantification. In contrast, MALDI MSI can provide spatial specificity by directly detecting the compound of interest at specific coordinates in the tissue section and the "microscopic" transport process of the drug in internal tissue can be observed precisely.

In the present study, a total of 21 mice were divided into 3 batches and used in the distribution study for octreotide based on the iMScope system. After i.g. administration of octreotide at a dose of 50 mg/kg, the mice were sacrificed at 10, 20, 40, 60, 120, 240 and 360 min under anesthesia (n=3 for each time point). The spatial distribution of octreotide in stomach section was performed under a lateral resolution at 50 μm and small pixel size at 5 μm. The representative stomach images determined by iMScope from the first batch of mice are shown in Figure 6. Obviously, stomach mucosa and musculature could be clearly distinguished by the CCD camera with magnification at X20 **(Fig. 6 (A1, B1, C1, D1 and E1))**. The microspotted

quantitative MALDI MS image of octreotide in the stomach section revealed that octreotide mainly concentrated in the gastric mucosal layer within 10 min to 40 min post dose (**Fig. 6 (A2, B2, and C2)**). As time went by, octreotide transported from the mucosal layer to the muscle side gradually, and the amount of octreotide in the musculature layer collected at 20 and 40 min was much more than that collected at 10 min despite the concentration gradient between the gastric mucosa and the musculature still existed. For the stomach specimen collected at 60 min, the signal intensity of octreotide in the mucosal layer was similar to that in the musculature layer, and the average signal intensity was quite low compared to that collected at 10 to 40 min post dose (**Fig. 6D2**). Subsequently, octreotide continued to be eliminated from the stomach quickly and the average signal intensity of octreotide in the stomach collected at 120 min was reduced to 1/4 of that collected at 60 min (**Fig. 6E2**). Then, the average intensity ratio of octreotide and IS in the ROIs (1.9 mm × 1.3 mm) of stomach sections at each time point were used to characterize the relative exposure levels of octreotide in the mouse stomach. The representative plot of relative intensity ratio – time profile is shown in **Fig. 6F**, and the mean relative intensity ratio - time curve with error bars is shown in Figure 4SA (n=3). The T_{max} of octreotide appeared at 10 min, and the $t_{1/2}$ was calculated as 28 min by Phoenix WinNonlin software. This is the first report of octreotide distribution and elimination with high-spatial precision and mass spectrometric specificity obtained based on the iMScope, which was characterized by high spatial resolution and excellent quantitative capability.

3.6. Quantitative IMS of Octreotide in Intestinal Tissue

In order to cover the entire transaction of the mouse intestine, the imaging was performed under a lateral resolution of 200 μm and pixel size of 10 μm. Meanwhile, 2.4 mm × 2.4 mm regions of each intestinal section were selected to perform the imaging experiment (**Fig. 7A1, B1…F1**). The microspotted quantitative iMScope images (**Fig. 7A2, B2…F2**) revealed the distribution and elimination pattern of octreotide in the intestinal section after ig oral administration of octreotide at a dose of 50 mg/kg. Obviously, the MS imaging of octreotide matched well with the shape of the intestine and no signal was detected in the microspots surrounding the tissue section. The average intensity ratio of octreotide and IS was adopted to

quantitatively describe the relative exposure levels of octreotide in the gastrointestinal tract. The representative plot of relative intensity ratio – time profile is shown in **Fig. 7G**, and the mean relative intensity ratio - time curve with error bars is shown in Figure 4SB (n=3). Obviously, the exposure amount of octreotide in intestine collected at 20, 40 and 60 min were much higher than those collected at 120, 240 and 360 min, which indicated that octreotide could distribute to the intestine quickly after being orally administrated to mice. The absorption peak time (T_{max}) appeared at 40 min and half-life time ($t_{1/2}$) was calculated as 37.7 min according the elimination rate of octreotide in mouse intestine. The pharmacokinetic parameters of octreotide were further confirmed via comparing the results from a piece of the same intestine analyzed by LC-MS/MS (**Fig. S5)**. Similarly, the T_{max} of octreotide detected by LC-MS/MS appeared at 40 min and the $t_{1/2}$ was calculated as 35.6 min by Phoenix WinNonlin software. No significant difference was found between these two sets of data. Therefore, iMScope could provide identical pharmacokinetic parameters as those obtained from the typical pharmacokinetic assay based on absolute quantitative analysis.

4. CONCLUSIONS

The high resolution iMScope was first applied to visually examine the distribution and elimination patterns of octreotide in mouse gastrointestinal tract. In this process, iMScope, the optical microscope in combination with the AP-MALDI-QIT-TOF, was found to offer several advantages, typically including retrospective “post-targeted” analysis, high spatial resolution (within 5-10 μm spatial resolution), excellent quantitative ability, high data collection rate and less probability of false positives and negatives. Besides, the AP ion-source chamber in iMScope system could efficiently shorten the sample preparation time, which is especially important for the pharmacokinetic study of large sample number. During quantitative analysis of iMScope, an ideal internal standard can significantly reduce several adverse factors such as matrix effect, tissue heterogeneity, signal inconsistency, *etc*. Lanreotide, a structural analogue of octreotide, was used as internal standard for octreotide due to their similar molecular weight, amino acid sequence, ionization characteristics, especially for its improvement on the quantitative ability of iMScope for

octreotide. Furthermore, ultra pure water and several kinds of organic solvents, including acetone, ethyl acetate, ISO alcohol and acetonitrile, were used to wash the tissue sections in the process of the method development. The results showed that washing tissue specimen would inevitably lead to a decline in recovery along with the spatial migration of the analytes, although washing can decrease the matrix effect to some extent.

For a pharmacokinetic study, absolute quantification is essential, but some important pharmacokinetic parameters can still be obtained based on relative quantitative analysis. In the present study, microspotted pixel-to-pixel quantitative iMScope provided a relative amount of octreotide presented in a thin stomach/intestine section, while preserving the original spatial distribution characteristics. This methodology, on the one hand, clearly visualized the transport process of octreotide from the mucosa layer to the muscle side in mouse stomach. On the other hand, it enabled the calculation of key pharmacokinetic parameters (T_{max} and $t_{1/2}$) of octreotide in the mouse gastrointestinal tract based on the relative exposure approach. Comparisons to the LC-MS/MS data confirmed that the relative quantification based on iMScope was reliable and practicable in drug pharmacokinetic study.

Acknowledgments

This study was supported by the National Nature Science Foundation (81273589, 81573559, 81374054, 81530098), the outstanding youth fund of State Key Laboratory of Natural Medicines (SKLNMZZJQ201602). We thank Elaine Kennedy (technician of Virginia Commonwealth University) for her linguistic assistance during the preparation of this manuscript.

References

[1] S. Forest, J. Breault-Turcot, P. Chaurand, J.F. Masson. Surface Plasmon Resonance Imaging-MALDI-TOF Imaging Mass Spectrometry of Thin Tissue Sections. Anal. Chem. 88 (2016) 2072-2079.

[2] J. Sekuła, J. Nizioł, W. Rode, T. Ruman. Gold nanoparticle-enhanced target (AuNPET) as universal solution for laser desorption/ionizationmass spectrometry analysis and imaging of low molecular weight compounds. Anal. Chim. Acta. 875 (2015) 61-72.

[3] L.R. Rodrigues, D.N. de Oliveira, M.S. Ferreira, R.R. Catharino. In situ assessment of atorvastatin impurity using MALDI mass spectrometry imaging (MALDI-MSI). Anal. Chim. Acta. 818 (2014) 32-38.

[4] Y. Gut, M. Boiret, L. Bultel, T. Renaud, A. Chetouani, A. Hafiane, Y.M. Ginot, R. Jennane. Application of chemometric algorithms to MALDI mass spectrometry imaging of pharmaceutical tablets. J. Pharm. Biomed. Anal. 105 (2015) 91-100.

[5] Y. Li, B. Shrestha, A. Vertes. Atmospheric pressure infrared MALDI imaging mass spectrometry for plant metabolomics. Anal. Chem. 80 (2008) 407-420.

[6] K. Dreisewerd, Recent methodological advances in MALDI mass spectrometry, Anal. Bioanal. Chem. 406 (2014) 2261-2278.

[7] P.C. Kooijman, S.J. Kok, J.J. Weusten, M. Honing. Independent assessment of matrix-assisted laser desorption/ionization mass spectrometry (MALDI-MS) sample preparation quality: A novel statistical approach for quality scoring. Anal. Chim. Acta. 919 (2016) 1-10.

[8] S. Vens-Cappell, I.U. Kouzel, H. Kettling, J. Soltwisch, A. Bauwens, S. Porubsky, J. Muthing, K. Dreisewerd, On-Tissue Phospholipase C Digestion for Enhanced MALDI-MS Imaging of Neutral Glycosphingolipids, Anal. Chem. 88 (2016) 5595-5599.

[9] K. Takahashi, T. Kozuka, A. Anegawa, A. Nagatani, T. Mimura. Development and Application of a High-Resolution Imaging Mass Spectrometer for the Study of Plant Tissues. Plant Cell Physiol. 56 (2015) 1329-1338.

[10] J.M. Spraggins, D.G. Rizzo, J.L. Moore, M.J. Noto, E.P. Skaar, R.M. Caprioli. Next-generation technologies for spatial proteomics: Integrating ultra-high speed MALDI-TOF and high mass resolution MALDI FTICR imaging mass spectrometry for protein analysis. Proteomics. 16 (2016) 1678-1689.

[11] J.M. Spraggins, D.G. Rizzo, J.L. Moore, K.L. Rose, N.D. Hammer, E.P. Skaar, R.M. Caprioli. MALDI FTICR IMS of Intact Proteins: Using Mass Accuracy to Link Protein Images with Proteomics Data. J. Am. Soc. Mass Spectrom. 26 (2015) 974-985.

[12] S. Guo, L. Qiu , Y. Wang , X. Qin, H. Liu, M. He, Y. Zhang, Z. Li, X. Chen.

Tissue imaging and serum lipidomic profiling for screening potential biomarkers of thyroid tumors by matrix-assisted laser desorption/ionization-Fourier transform ion cyclotron resonance mass spectrometry. Anal. Bioanal. Chem. 406 (2014) 4357-470.

[13] C.L. Carter, J.W. Jones, A.M. Farese, T.J. MacVittie, M.A. Kane, Inflation-Fixation Method for Lipidomic Mapping of Lung Biopsies by Matrix Assisted Laser Desorption/Ionization-Mass Spectrometry Imaging, Anal. Chem. 88 (2016) 4788-4794.

[14] R. Jirasko, M. Holcapek, M. Kunes, A. Svatos, Distribution study of atorvastatin and its metabolites in rat tissues using combined information from UHPLC/MS and MALDI-Orbitrap-MS imaging, Anal. Bioanal. Chem. 406 (2014) 4601-4610.

[15] T.E. Fehniger, A. Vegvari, M. Rezeli, K. Prikk, P. Ross, M. Dahlback, G. Edula, R. Sepper, G. Marko-Varga, Direct demonstration of tissue uptake of an inhaled drug: proof-of-principle study using matrix-assisted laser desorption ionization mass spectrometry imaging, Anal. Chem. 83 (2011) 8329-8336.

[16] B. Prideaux, V. Dartois, D. Staab, D.M. Weiner, A. Goh, L.E. Via, C.E. Barry, 3rd, M. Stoeckli, High-sensitivity MALDI-MRM-MS imaging of moxifloxacin distribution in tuberculosis-infected rabbit lungs and granulomatous lesions, Anal. Chem. 83 (2011) 2112-2118.

[17] R.J. Goodwin, A. Nilsson, D. Borg, P.R. Langridge-Smith, D.J. Harrison, C.L. Mackay, S.L. Iverson, P.E. Andren, Conductive carbon tape used for support and mounting of both whole animal and fragile heat-treated tissue sections for MALDI MS imaging and quantitation, J. Proteomics, 75 (2012) 4912-4920.

[18] C.W. Chumbley, M.L. Reyzer, J.L. Allen, G.A. Marriner, L.E. Via, C.E. Barry, 3rd, R.M. Caprioli, Absolute Quantitative MALDI Imaging Mass Spectrometry: A Case of Rifampicin in Liver Tissues, Anal. Chem. 88 (2016) 2392-2398.

[19] A. Nilsson, R.J. Goodwin, M. Shariatgorji, T. Vallianatou, P.J. Webborn, P.E. Andren, Mass spectrometry imaging in drug development, Anal. Chem. 87 (2015) 1437-1455.

[20] Y. Liang, G. Wang, L. Xie, L. Sheng, Recent development in liquid chromatography/mass spectrometry and emerging technologies for metabolite identification, Curr. Drug Metab. 12 (2011) 329-344.

[21] M. Pfannmöller, H. Flügge, G. Benner, I. Wacker, C. Sommer, M. Hanselmann, S. Schmale, H. Schmidt, F.A. Hamprecht, T. Rabe, W. Kowalsky, R.R. Schröder. Visualizing a

homogeneous blend in bulk heterojunction polymer solar cells by analytical electron microscopy. Nano. Lett. 11 (2011) 3099-3107.

[22] T.C. Baker, J. Han, C.H. Borchers. Recent advancements in matrix-assisted laser desorption/ionization mass spectrometry imaging. Curr Opin Biotechnol. 43 (2016) 62-69.

[23] W. Chao, B.D. Harteneck, J.A. Liddle, E.H. Anderson, D.T. Attwood. Soft X-ray microscopy at a spatial resolution better than 15 nm. Nature. 435 (2005) 1210-1213.

[24] R.D. Addie, B. Balluff, J.V. Bovee, H. Morreau, L.A. McDonnell, Current State and Future Challenges of Mass Spectrometry Imaging for Clinical Research, Anal. Chem. 87 (2015) 6426-6433.

[25] K.A. Youdim, K.C. Saunders, A review of LC-MS techniques and high-throughput approaches used to investigate drug metabolism by cytochrome P450s, J. Chromatogr. B. 878 (2010) 1326-1336.

[26] A. Kamel, C. Prakash, High performance liquid chromatography/atmospheric pressure ionization/tandem mass spectrometry (HPLC/API/MS/MS) in drug metabolism and toxicology, Curr. Drug Metab. 7 (2006) 837-852.

[27] M. El Amrani, M.P. van den Broek, C. Gobel, E.M. van Maarseveen, Quantification of active infliximab in human serum with liquid chromatography-tandem mass spectrometry using a tumor necrosis factor alpha -based pre-analytical sample purification and a stable isotopic labeled infliximab bio-similar as internal standard: A target-based, sensitive and cost-effective method, J. Chromatogr. A.1454 (2016) 42-48.

[28] T. Harada, A. Yuba-Kubo, Y. Sugiura, N. Zaima, T. Hayasaka, N. Goto-Inoue, M. Wakui, M. Suematsu, K. Takeshita, K. Ogawa, Y. Yoshida, M. Setou, Visualization of volatile substances in different organelles with an atmospheric-pressure mass microscope, Anal. Chem. 81 (2009) 9153-9157.

[29] N. Kurabe, H. Igarashi, I. Ohnishi, S. Tajima, Y. Inoue, Y. Takahashi, M. Setou, H. Sugimura, Visualization of sphingolipids and phospholipids in the fundic gland mucosa of human stomach using imaging mass spectrometry, World J. Gastrointestinal Pathophysiol. 7 (2016) 235-241.

[30] S. Shimma, H.O. Kumada, H. Taniguchi, A. Konno, I. Yao, K. Furuta, T. Matsuda, S. Ito, Microscopic visualization of testosterone in mouse testis by use of imaging mass spectrometry, Anal. Bioanal. Chem. (2016).

[31] X. Zhang, Z. Lin, J. Fang, M. Liu, Y. Niu, S. Chen, H. Wang, An on-line high-performance liquid chromatography-diode-array detector-electrospray ionization-ion-trap-time-of-flight-mass spectrometry-total antioxidant capacity detection system applying two antioxidant methods for activity evaluation of the edible flowers from Prunus mume, J. Chromatogr. A. 1414 (2015) 88-102.

[32] M. Fraga, N. Vilarino, M.C. Louzao, D.A. Fernandez, M. Poli, L.M. Botana, Detection of palytoxin-like compounds by a flow cytometry-based immunoassay supported by functional and analytical methods, Anal. Chim. Acta. 903 (2016) 1-12.

[33] H. Hao, N. Cui, G. Wang, B. Xiang, Y. Liang, X. Xu, H. Zhang, J. Yang, C. Zheng, L. Wu, P. Gong, W. Wang, Global detection and identification of nontarget components from herbal preparations by liquid chromatography hybrid ion trap time-of-flight mass spectrometry and a strategy, Anal. Chem. 80 (2008) 8187-8194.

[34] S.B. Guo, Q. Li, Z.J. Duan, Q.M. Wang, Q. Zhou, X.Y. Sun, Octreotide attenuates liver fibrosis by inhibiting hepatic heme oxygenase-1 expression, Molecular medicine reports, 11 (2015) 83-90.

[35] D.X. Zhou, H.B. Zhou, Q. Wang, S.S. Zou, H. Wang, H.P. Hu, The effectiveness of the treatment of octreotide on chylous ascites after liver cirrhosis, Digest. Dis. Sci. 54 (2009) 1783-1788.

[36] Q. Wang, Y. Liang, T. Rao, L. Xie, W. Ye, H. Fu, L. Zhou, R. Xing, Y. Shao, J. Xiao, D. Kang, G. Wang, PK study of octreotide based on LC-MS/MS combining protein precipitation and impurity extraction technique, Bioanal. 7 (2015) 885-894.

[37] I. Fournier, C. Marinach, J.C. Tabet, G. Bolbach, Irradiation effects in MALDI, ablation, ion production, and surface modifications. Part II. 2,5-dihydroxybenzoic acid monocrystals, J. Am. Soc. Mass Spectr. 14 (2003) 893-899.

[38] H. Keshishian, T. Addona, M. Burgess, D.R. Mani, X. Shi, E. Kuhn, M.S. Sabatine, R.E. Gerszten, S.A. Carr, Quantification of cardiovascular biomarkers in patient plasma by targeted mass spectrometry and stable isotope dilution, Mol. Cell. Proteomics. 8 (2009) 2339-2349.

[39] P.J. Boersema, L.Y. Foong, V.M. Ding, S. Lemeer, B. van Breukelen, R. Philp, J. Boekhorst, B. Snel, J. den Hertog, A.B. Choo, A.J. Heck, In-depth qualitative and quantitative profiling of tyrosine phosphorylation using a combination of phosphopeptide immunoaffinity purification and stable isotope dimethyl labeling, Mol. Cell. Proteomics. 9 (2010) 84-99.

[40] X. Wang, J. Han, A. Chou, J. Yang, J. Pan, C.H. Borchers. Hydroxyflavones as a new family of matrices for MALDI tissue imaging. Anal. Chem. 85 (2013) 7566-7573.

[41] S. Shimma, Y. Takashima, J. Hashimoto, K. Yonemori, K. Tamura, A. Hamada. Alternative two - step matrix application method for imaging mass spectrometry to avoid tissue shrinkage and improve ionization efficiency. J. Mass Spectrom, 48 (2013) 1285-1290.

[42] S. Shimma, H.O. Kumada, H. Taniguchi, A. Konno, I. Yao, K. Furuta, T. Matsuda, S. Ito. Microscopic visualization of testosterone in mouse testis by use of imaging mass spectrometry. Anal. Bioanal. Chem. (2016) 1-9.

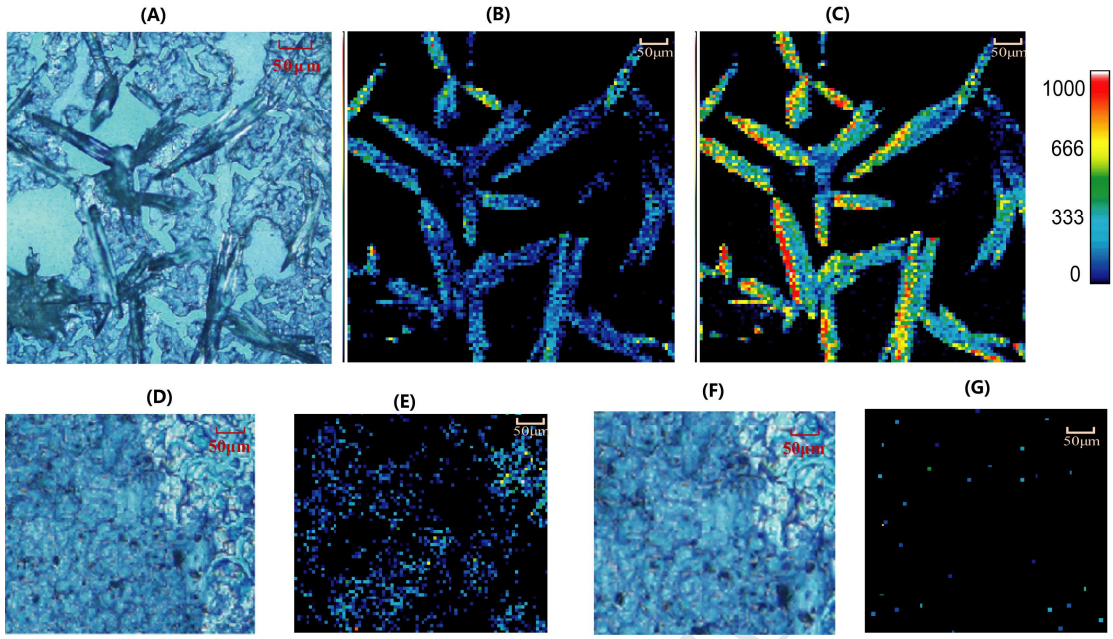

Fig. 1 Imaging MS analysis of the octreotide and lanreotide (internal standard) in mouse stomach generated by LDI-QIT-TOF-IMS (The scale bar was 50 μm). (a) magnified view of the tissue after spraying DHB as matrix, (b) imaging MS analysis of octreotide at *m/z* 1019.44 with DHB as the matrix, (c) imaging MS analysis of lanreotide at *m/z* 1096.47 with DHB as the matrix, (d) magnified view of the tissue after spraying CHCA as matrix, (e) imaging MS analysis of octreotide at *m/z* 1019.44 with CHCA as the matrix, (f) magnified view of the tissue after spraying SA as matrix, (g) imaging MS analysis of octreotide at *m/z* 1019.44 with SA as the matrix.

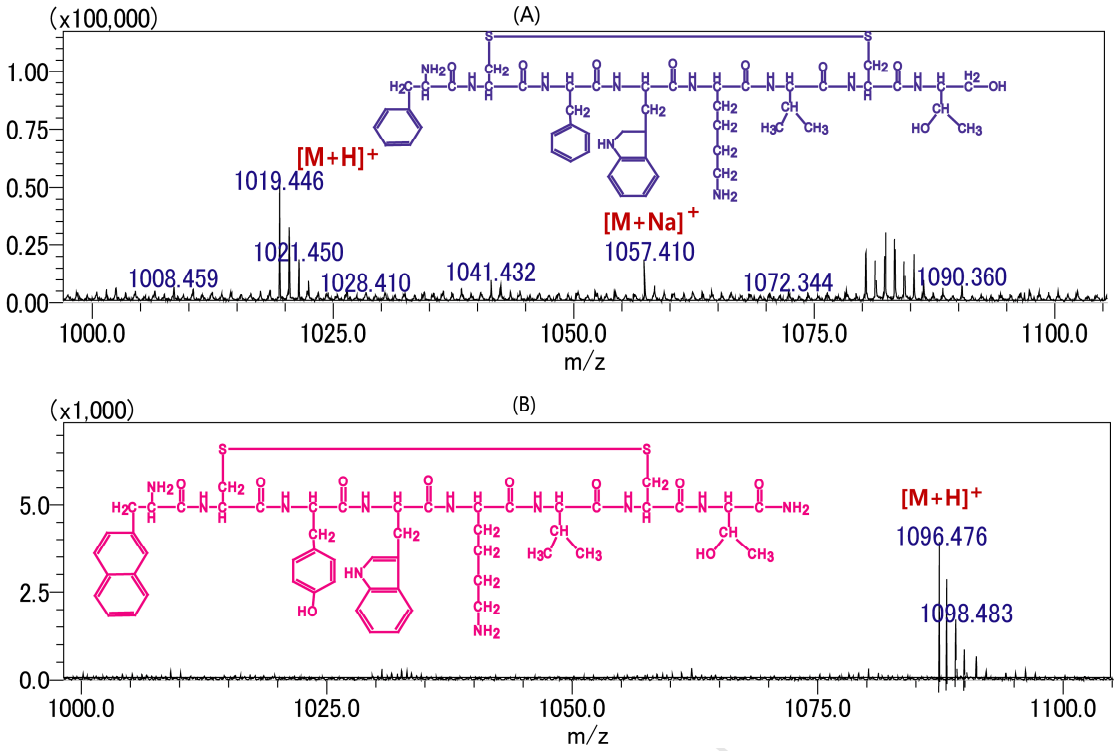

Fig. 2 The structures and mass spectrum of octreotide and lanreotide (internal standard). A: octreotide; B: lanreotide.

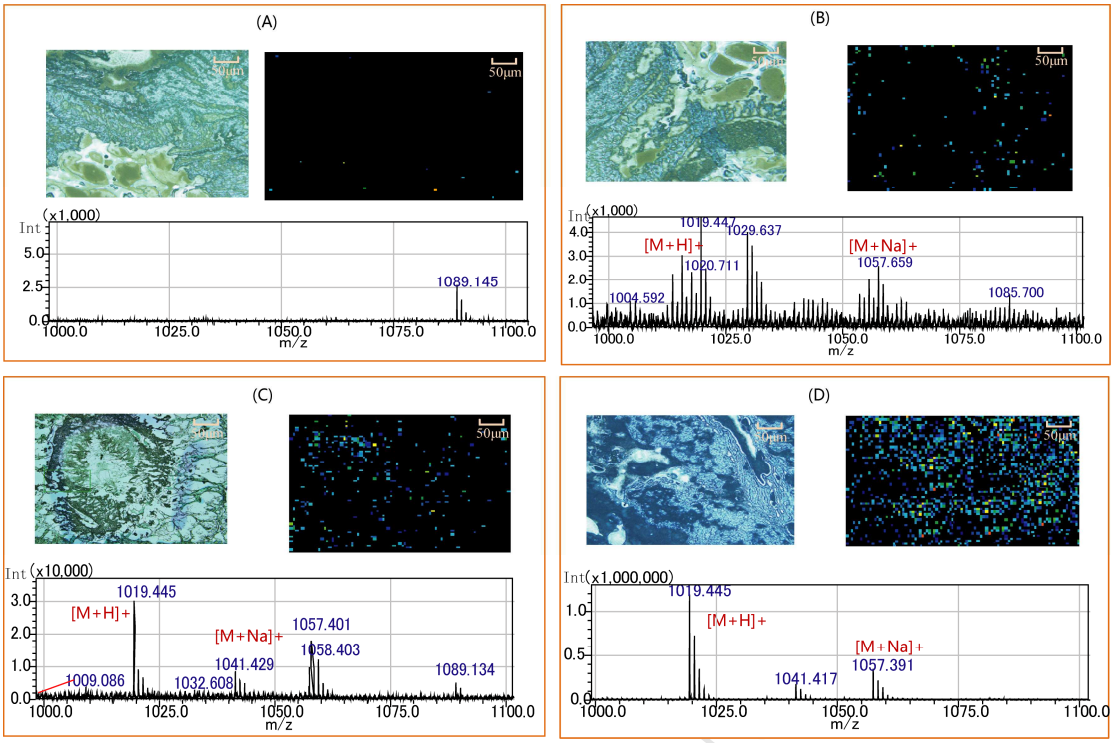

Fig. 3 Imaging MS analysis of the octreotide generated by AP-MALDI-QIT-TOF-IMScope under 4 different matrix spraying modes (The scale bar was 50 μm). (a) sublimation, (b) sublimation & recrystallization, (c) airbrushing, (d) sublimation & airbrushing.

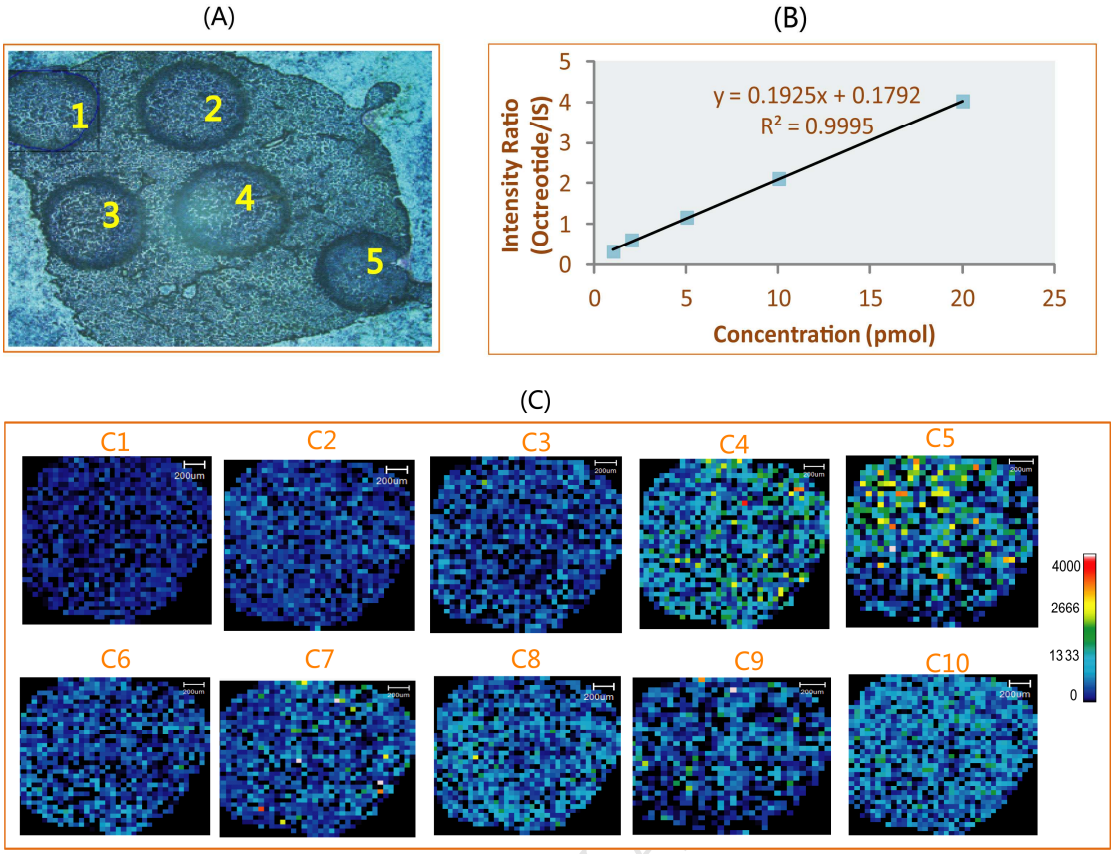

Fig. 4 Calibration curves of octreotide constructed by plotting the average intensity ratios (octreotide / lanreotide) against the concentrations in mouse stomach section determined based on LDI-QIT-TOF-IMS (The scale bar was 50 μm). (a) optical image of the mouse tissue acquired by microscope via magnifying for 20X, (b) calibration curves of octreotide in mouse intestinal section , (c) imaging MS analysis of octreotide at 5 concentration levels (c1: 1 pmol, c2: 2 pmol, c3: 5 pmol, c4: 10 pmol, c5: 20 pmol) mixed with 10 pmol lanreotide which was used for the calibration of intensities of octreotide at 1, 2, 5, 10 and 20 pmol, respectively (c6 ~ c10).

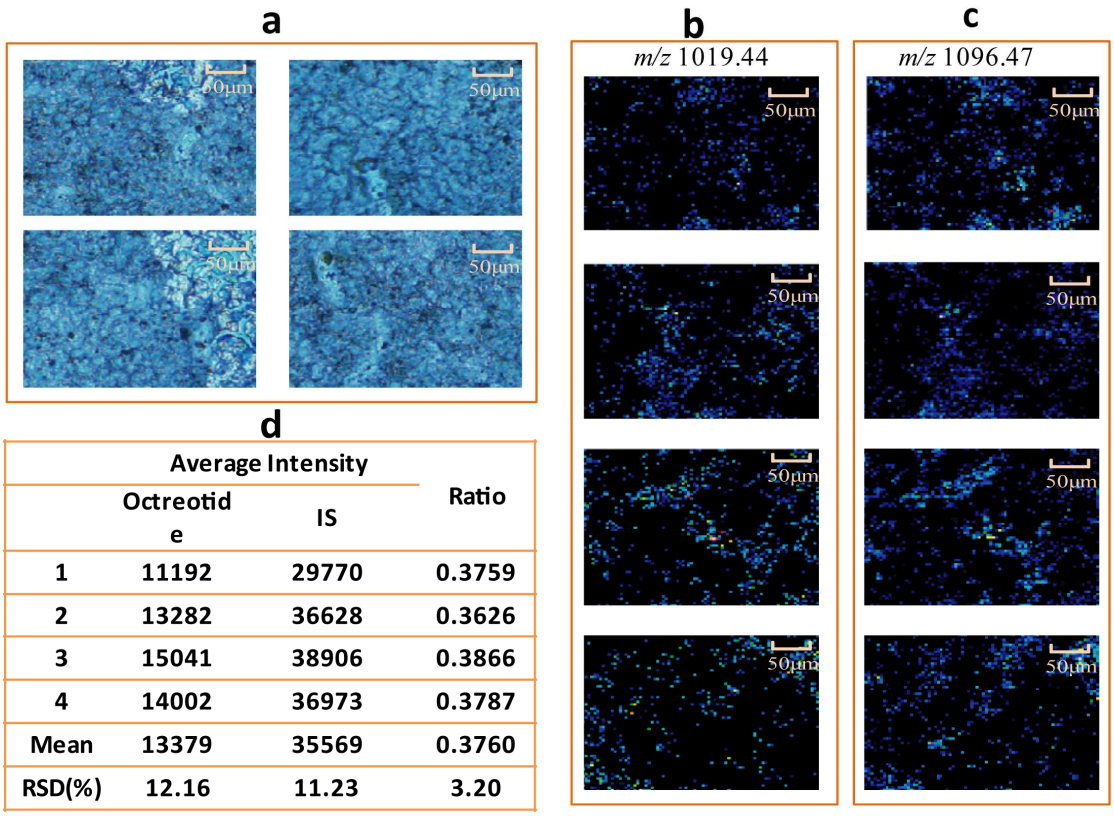

d

	Average Intensity		Ratio
	Octreotide	IS	
1	11192	29770	0.3759
2	13282	36628	0.3626
3	15041	38906	0.3866
4	14002	36973	0.3787
Mean	13379	35569	0.3760
RSD(%)	12.16	11.23	3.20

Fig. 5 The average intensity ratio of octreotide and IS in four sections of blank stomach tissue covered by the same concentration of the analytes determined based on AP-MALDI-QIT-TOF-iMScope (The scale bar was 50 μm). (a) optical image of mouse stomach section spiked with the standard solution of octreotide acquired by the CCD camera (magnification, × 20) which embedded in the iMScope system; (b) imaging MS analysis of octreotide at *m/z* 1019.44; (c) imaging MS analysis of lanreotide at *m/z* 1096.47; (d) precision data analysis for octreotide.

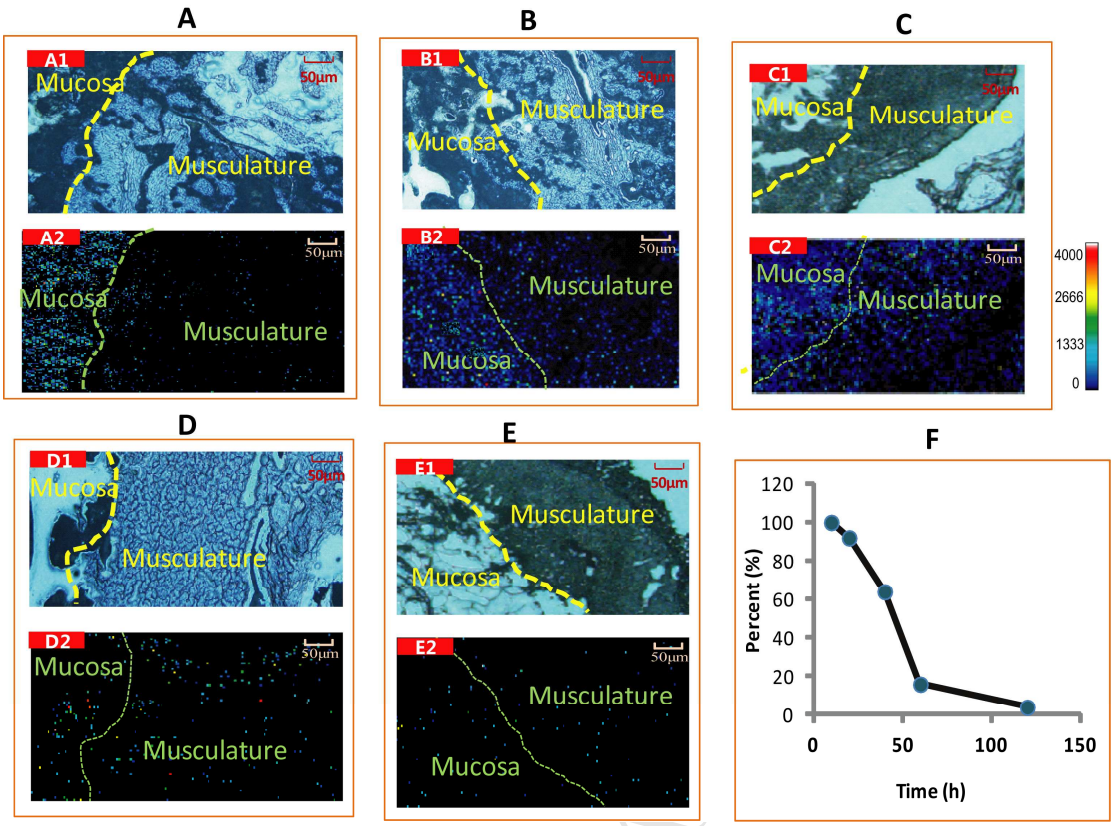

Fig. 6 The spatial distribution and elimination of octreotide in mouse stomach after intragastrical administration of octreotide at a dose of 50 mg/kg (The scale bar was 50 μm). The spatial distribution of octreotide at 10 min (A), 20 min (B), 40 min (C), 60 min (D) and 120 min (E) post dose (A1, B1~E1: magnified optical image of the mouse stomach; A2, B2~E2: imaging MS analysis of octreotide).

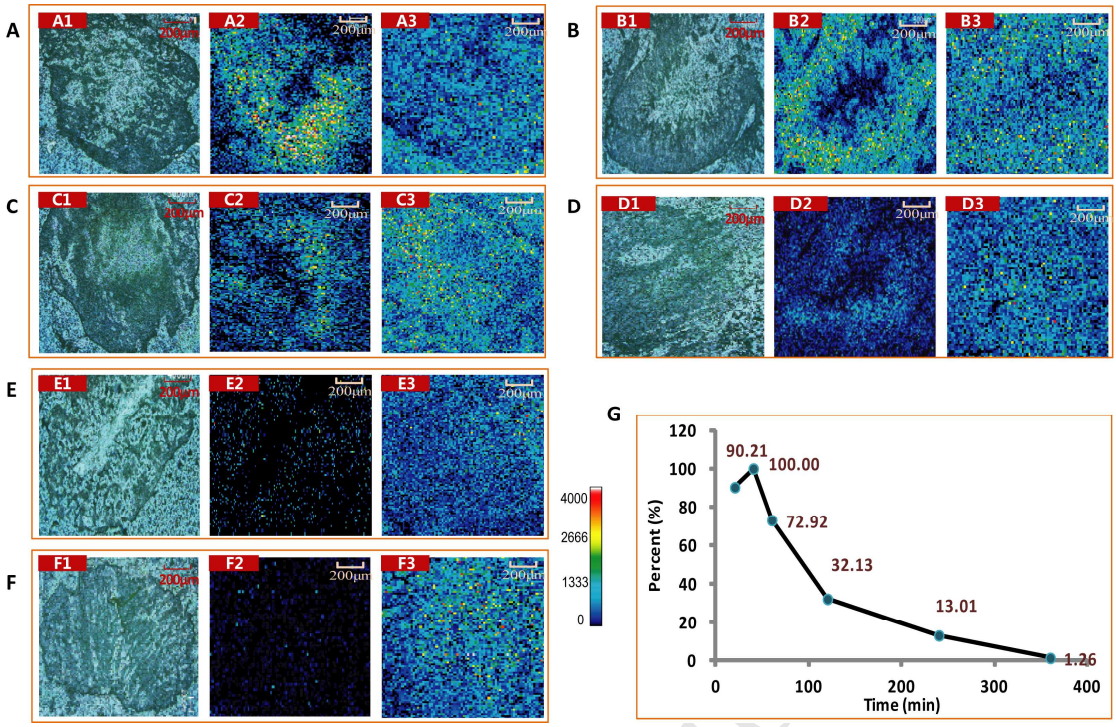

Fig. 7 The distribution and elimination of octreotide in mouse intestinal after intragastrical administration of octreotide at a dose of 50 mg/kg (The scale bar was 200 μm). The distribution of octreotide at 20 min (A), 40 min (B), 60 min (C), 120 min (D), 240 min (E) and 360 min (F) post dose (A1, B1~F1: magnified view of the mouse intestinal; A2, B2~F2: imaging MS analysis of octreotide; A3, B3~F3: imaging MS analysis of lanreotide for the calibration of intensities of octreotide at 20, 40, 60, 120, 240 and 360 min in mouse intestinal, respectively). (G) the time-concentration curve of octreotide in mouse intestinal.

Figure Captions

Fig. 1 Imaging MS analysis of the octreotide and lanreotide (internal standard) in mouse stomach generated by LDI-QIT-TOF-IMS (The scale bar was 50 μm). (a) magnified view of the tissue after spraying DHB as matrix, (b) imaging MS analysis of octreotide at *m/z* 1019.44 with DHB as the matrix, (c) imaging MS analysis of lanreotide at *m/z* 1096.47 with DHB as the matrix, (d) magnified view of the tissue after spraying CHCA as matrix, (e) imaging MS analysis of octreotide at *m/z* 1019.44 with CHCA as the matrix, (f) magnified view of the tissue after spraying SA as matrix, (g) imaging MS analysis of octreotide at *m/z* 1019.44 with SA as the matrix.

Fig. 2 The structures and mass spectrum of octreotide and lanreotide (internal standard). A: octreotide; B: lanreotide.

Fig. 3 Imaging MS analysis of the octreotide generated by AP-MALDI-QIT-TOF-IMScope under 4 different matrix coating modes (The scale bar was 50 μm). (a) sublimation, (b) sublimation & recrystallization, (c) airbrushing, (d) sublimation & airbrushing.

Fig. 4 Calibration curves of octreotide constructed by plotting the average intensity ratios (octreotide / lanreotide) against the concentrations in mouse stomach section determined based on LDI-QIT-TOF-IMS (The scale bar was 50 μm). (a) optical image of the tissue acquired by microscope via magnifying for 20X, (b) calibration curves of octreotide in mouse intestinal section , (c) imaging MS analysis of octreotide at 5 concentration levels (c1: 1 pmol, c2: 2 pmol, c3: 5 pmol, c4: 10 pmol, c5: 20 pmol) mixed with 10 pmol lanreotide which was used for the calibration of intensities of octreotide at 1, 2, 5, 10 and 20 pmol, respectively (c6 ~ c10).

Fig. 5 The average intensity ratio of octreotide and IS in four sections of blank stomach tissue covered by the same concentration of the analytes determined based on AP-MALDI-QIT-TOF-iMScope (The scale bar was 50 μm). (a) optical image of mouse stomach section spiked with the standard solution of octreotide acquired by the CCD camera (magnification,×40) which embedded in the iMScope system; (b) imaging MS analysis of octreotide at *m/z* 1019.44; (c) imaging MS analysis of lanreotide at *m/z* 1096.47; (d) precision data analysis for octreotide.

Fig. 6 The spatial distribution and elimination of octreotide in mouse stomach after intragastrical administration of octreotide at a dose of 50 mg/kg. The spatial distribution of octreotide at 10 min (A), 20 min (B), 40 min (C), 60 min (D) and 120 min (E) post dose (A1, B1~E1: magnified view of the mouse stomach; A2, B2~E2: imaging MS analysis of octreotide). (F) the

time-concentration curve of octreotide in mouse stomach.

Fig. 7 The distribution and elimination of octreotide in mouse intestinal after intragastrical administration of octreotide at a dose of 50 mg/kg (The scale bar was 200 μm). The distribution of octreotide at 20 min (A), 40 min (B), 60 min (C), 120 min (D), 240 min (E) and 360 min (F) post dose (A1, B1~F1: magnified view of the mouse intestinal; A2, B2~F2: imaging MS analysis of octreotide; A3, B3~F3: imaging MS analysis of lanreotide for the calibration of intensities of octreotide at 20, 40, 60, 120, 240 and 360 min in mouse intestinal, respectively). (G) the time-concentration curve of octreotide in mouse intestinal.

HIGHLIGHTS

- **IMScope was first validated and applied to visualize drug dynamics.**
- **A novel relative exposure was developed for pharmacokinetic study.**
- **The octreotide transport process from mucosal to muscle was imaged.**
- **The distribution and elimination of octreotide was studied *in vivo*.**